Biochem. J. (2014) **463**, 239–248 (Printed in Great Britain) doi:10.1042/BJ20140306

Enantioselective microbial synthesis of the indigenous natural product (−)-α-bisabolol by a sesquiterpene synthase from chamomile (*Matricaria recutita*)

Young-Jin SON*, Moonhyuk KWON†, Dae-Kyun RO†[1] and Soo-Un KIM*‡[1]

*Department of Agricultural Biotechnology and Research Institute of Agriculture and Life Sciences, Seoul National University, Seoul 151-921, South Korea
†Department of Biological Sciences, University of Calgary, Calgary, Canada, T2N 1N4
‡School of Gardening and Horticulture, Yangtze University, Jingzhou, Hubei 434023, China

(−)-α-Bisabolol, a sesquiterpene alcohol, is a major ingredient in the essential oil of chamomile (*Matricaria recutita*) and is used in many health products. The current supply of (−)-α-bisabolol is mainly dependent on the Brazilian candeia tree (*Eremanthus erythropappus*) by distillation or by chemical synthesis. However, the distillation method using the candeia tree is not sustainable, and chemical synthesis suffers from impurities arising from undesirable α-bisabolol isomers. Therefore enzymatic synthesis of (−)-α-bisabolol is a viable alternative. In the present study, a cDNA encoding (−)-α-bisabolol synthase (*MrBBS*) was identified from chamomile and used for enantioselective (−)-α-bisabolol synthesis in yeast. Chamomile *MrBBS* was identified by Illumina and 454 sequencing, followed by activity screening in yeast. When *MrBBS* was expressed in yeast, 8 mg of α-bisabolol was synthesized *de novo* per litre of culture. The structure of purified α-bisabolol was elucidated as (*S*,*S*)-α-bisabolol [or (−)-α-bisabolol]. Although MrBBS possesses a putative chloroplast-targeting peptide, it was localized in the cytosol, and a deletion of its N-terminal 23 amino acids significantly reduced its stability and activity. Recombinant MrBBS showed kinetic properties comparable with those of other sesquiterpene synthases. These data provide compelling evidence that chamomile MrBBS synthesizes enantiopure (−)-α-bisabolol as a single sesquiterpene product, opening a biotechnological opportunity to produce (−)-α-bisabolol.

Key words: bisabolol, candeia, chamomile, metabolic engineering, terpene synthase, yeast.

INTRODUCTION

Terpenoids (or isoprenoids) are the largest and structurally most diverse group of secondary metabolites, with more than 55 000 listed compounds [1]. In Nature, terpenoids have essential roles, such as those involved in protein prenylation (e.g. RAS prenylation), plant hormonal regulation (e.g. gibberellin, brassinosteroids, cytokinin and abscisic acid), photosynthetic light harvesting (e.g. carotenoid and chlorophyll), and respiratory electron transport (e.g. ubiquinone) [2–4]. Terpenoids often function as toxins, growth inhibitors or deterrents to protect the producers from competing plants or herbivores [5]. Terpenoids also have been extensively exploited by humans for their beneficial functions as pharmaceuticals (e.g. paclitaxel and artemisinin), flavours and fragrance compounds (e.g. menthol, patchoulol and nootkatone) [6].

In Nature, terpenoids are synthesized from successive condensations of five-carbon building units. These are IPP (isopentenyl diphosphate) and its isomer, DMAPP (dimethyl allyl diphosphate), both of which are synthesized in two independent pathways: the cytosolic MVA (mevalonate) pathway and the plastidic MEP (2-C-methyl-D-erythritol 4-phosphate) pathway [3,7]. Starting with DMAPP, the head to tail condensation reaction is catalysed by prenyltransferase, and one to three IPP units are added to yield three prenyl diphosphate molecules: C_{10} GPP (geranyl diphosphate), C_{15} FPP (farnesyl diphosphate) and C_{20} GGPP (geranylgeranyl diphosphate). These prenyl diphosphates are converted by TPS (terpene synthase) into various terpene hydrocarbons [8,9]. Isoprenoids are classified according to the number of carbons as monoterpenes (C_{10}), sesquiterpenes (C_{15}) and diterpenes (C_{20}). As terpenes have multiple chiral centres and complex hydrocarbon backbones, chemical synthesis of terpenes is not usually practical, and hence the identification and utilization of unique TPSs are central in contemporary pharmaceutical and chemical industries [10].

Chamomile (*Matricaria recutita*) is one of the most commonly consumed herbal medicines [11]. The therapeutic values of chamomile come from its essential oil component, (−)-α-bisabolol [12]. (−)-α-Bisabolol, a sesquiterpene alcohol, is naturally occurring in the Brazilian candeia tree (*Eremanthus erythropappus*) and also in German chamomile (*Matricaria recutita*) [13,14]. This compound has been shown to possess various pharmaceutical activities (e.g. antibacterial, antiseptic and anti-inflammatory) and skin-soothing and -moisturizing properties [15–18]. At present, the majority of (−)-α-bisabolol, sold as 'natural α-bisabolol', is produced by distillation of candeia tree leaves [14]. However, sustainability of this Brazilian indigenous plant has raised an environmental issue in recent years

Abbreviations: DMAPP, dimethyl allyl diphosphate; EI, electron impact; FPP, farnesyl diphosphate; FPPS, FPP synthase; IPP, isopentenyl diphosphate; LdBBS, (+)-*epi*-α-bisabolol synthase from *Lippia dulcis*; MBP, maltose-binding protein; mono-TPS, monoterpene synthase; MrBBS, chamomile (*Matricaria recutita*) α-bisabolol synthase; MrTPS, chamomile (*Matricaria recutita*) TPS; MVA, mevalonate; NPP, nerolidyl diphosphate; qRT-PCR, quantitative reverse transcription–PCR; SC, synthetic complete; sesqui-TPS, sesquiterpene synthase; TPS, terpene synthase; TRX, thioredoxin.

[1] Correspondence may be addressed to either of these authors (email soounkim@snu.ac.kr or daekyun.ro@ucalgary.ca).

Nucleotide sequence of identified *Matricaria recutita* sesquiterpene synthases have been submitted to the DDBJ, EMBL, GenBank® and GSDB Nucleotide Sequence Databases with accession numbers: KJ020282 [MrTPS1, (−)-α-bisabolol synthase], KJ020284 (MrTPS4, bicyclogermacrene synthase) and KJ020283 (MrTPS6, β-farnesene synthase).

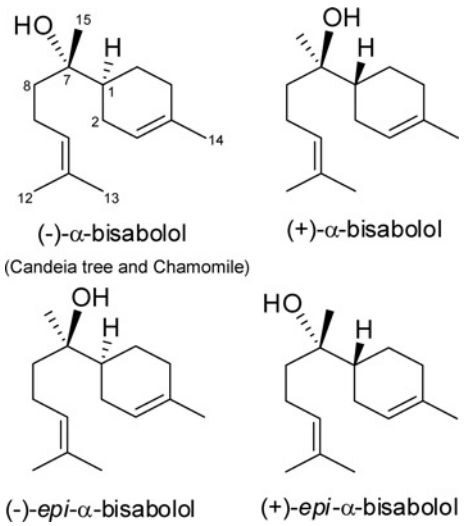

Figure 1 Structures of four α-bisabolol isomers

[19]. (−)-α-Bisabolol can be chemically synthesized, but the synthetic (−)-α-bisabolol contains other diastereomers [(+)-α-bisabolol and (+/−)-*epi*-α-bisabolol] and undesirable by-products from chemical synthesis procedures. Therefore synthetic production of 'natural identical' (−)-α-bisabolol requires an economically unfavourable purification procedure to achieve a high optical purity. Nonetheless, the synthetic supply of (−)-α-bisabolol and its stereoisomers have recently been replacing the natural (−)-α-bisabolol production from the Brazilian candeia tree.

α-Bisabolol possesses two chiral centres at C1 and C7 (Figure 1). Depending on the configuration of these two chiral carbons, four possible stereoisomers of α-bisabolols, (+/−)-α-bisabolol and (+/−)-*epi*-α-bisabolol, can be formed [20]. Previously, two α-bisabolol synthase genes were identified from Aztec herb (*Lippia dulcis*) and bacterium *Streptomyces citricolor*, and the products from their recombinant enzymes were elucidated as (+)-*epi*-α-bisabolol and (−)-*epi*-α-bisabolol respectively [21,22]. Although a specific configuration was not elucidated, one other α-bisabolol synthase was also found from *Artemisia annua* [23], and dual-functional bisabolene/α-bisabolol synthases which synthesize only a trace amount of α-bisabolol were isolated from *Arabidopsis* and *Santalolum* spp. [24,25]. To date, a sesqui-TPS (sesquiterpene synthase) synthesizing pure (−)-α-bisabolol as a single terpene product has not been identified.

From chamomile, five TPSs have recently been characterized [26]. However, (−)-α-bisabolol synthase was not included among the TPSs characterized from chamomile. In the present study, we identified a gene encoding chamomile α-bisabolol synthase (*MrBBS*) using next-generation (Illumina and 454) sequencing. This enzyme can synthesize enantiopure (−)-α-bisabolol as a single terpene product. Furthermore, as proof-of-concept, microbial and *in planta* production of (−)-α-bisabolol was demonstrated.

EXPERIMENTAL

Plant material

Chamomile (*M. recutita*) was grown in a phyto-chamber maintained with a 16 h light/8 h dark photoperiod at 23 °C. Stem, leaf, root and flower were harvested from 6-week-old *M. recutita*. *Nicotiana benthamiana* for transient expression experiments was grown for 5–6 weeks in a phyto-chamber with a 16 h light/8 h dark photoperiod at 23 °C.

DNA construct for yeast expression

Six TPS clones were amplified from 20 ng of cDNA using the primers listed in Supplementary Table S1 (http://www.biochemj.org/bj/463/bj4630239add.htm) (1–12). Amplified PCR products were cloned into pMD-20 (TaKaRa Bio), and cDNA sequences were confirmed by sequencing. The TPS cDNAs were digested using restriction enzymes and ligated into the respective restriction digestion sites of pESC-Leu2d vector. For fused MrBBS, MBP (maltose-binding protein), GST and TRX (thioredoxin) were amplified using primers 28–33 using templates of pMAL-c2X (NEB) pGEX-2T (GE Healthcare) and pET32a (Novagen) respectively. Amplified PCR products were digested appropriately and ligated to the N-terminus of MrBBS in pESC-Leu2d vector. To characterize each sesqui-TPS, the constructs and empty vector were separately transformed into the EPY300 yeast strain by the lithium acetate/PEG transformation method [27–29].

In vivo yeast characterization and bisabolol quantification

Transgenic yeast were inoculated in 2 ml of SC (synthetic complete) medium (supplemented with 2 % glucose and lacking methionine, histidine and leucine) and grown overnight at 30 °C. The transgenic yeast culture was diluted 50-fold into 30 ml of SC medium (with 1.8 % galactose, 0.2 % glucose, 2 mM methionine and lacking histidine and leucine). To sequester the volatile sesquiterpene product, 3 ml of dodecane was overlaid on to the culture, and incubated at 30 °C and 200 rev./min for 3 days. Cultures were transferred to a 50 ml Falcon tube and centrifuged at 3000 ***g*** for 5 min. The dodecane layer was separated and diluted 100-fold in hexane for GC–MS analysis. For quantification, the cultured medium was extracted with ethyl acetate and analysed by GC–FID (flame ionizer detector) (Shimadzu) against the calibration curve constructed from commercial (−)-α-bisabolol (Sigma) using the following temperature programme: initial temperature 60 °C (2 min hold), increase to 300 °C at 5 °C·min^{-1}, and 300 °C held for 10 min. The analysis was conducted using a ZB-5 GC column (0.25 μm film thickness, 0.25 mm×30 m) and nitrogen as a carrier gas at a flow rate of 1 ml·min^{-1}.

Protein expression in *Escherichia coli* and purification

To obtain recombinant MrBBS–His_6, the ORFs of full-length *MrBBS*, 23- or 52-residue-deleted *MrBBS* were cloned into pET21 vector (Novagen), using the Gibson assembly cloning kit (NEB) and the primers listed in Supplementary Table S1 (13–16). Recombinant pET21-MrBBS-His_6 construct was transformed into *E. coli* BL21 codon plus-RIL cells (Stratagene) and selected with ampicillin (100 μg·ml^{-1}) and chloramphenicol (36 μg·ml^{-1}). A single transformed colony was cultured in LB medium to a D_{600} of 0.5. *MrTPS* (chamomile TPS) expression was then induced with 0.4 mM IPTG by incubation at 17 °C for 16 h. The cells were harvested by centrifugation and resuspended in lysis buffer [20 mM Hepes (pH 7.6), 10 mM $MgCl_2$, 500 mM NaCl, 5 mM 2-mercaptoethanol, 20 mM imidazole, 10 % (w/v) glycerol and 1 mM PMSF]. After cell lysis by sonication and centrifugation at 4000 ***g*** for 10 min at 4 °C, the clear supernatant was loaded on to a 1 ml HisTrap HP column (GE Healthcare), which was pre-equilibrated with wash buffer [20 mM sodium phosphate (pH 7.4), 10 mM $MgCl_2$, 500 mM NaCl, 5 mM 2-mercaptoethanol, 20 mM imidazole and 15 % (w/v) glycerol].

After the column was washed with a 10-fold column volume of the wash buffer, the bound protein was eluted by a linear gradient of imidazole up to 500 mM. Protein in each fraction was confirmed using SDS/PAGE. Fractions containing the sesqui-TPS were pooled and dialysed at 4 °C for 24 h to remove imidazole.

In vitro enzyme assay and kinetics

For the *in vitro* enzyme assay, 500 μl of reaction mixture was prepared with 20 μg of purified recombinant protein, 100 μM FPP (Echelon Biosciences), 50 mM Tris/HCl (pH 7.5) and 10 mM $MgCl_2$. The mixture was incubated at 30 °C for 2 h, followed by extraction with 500 μl of pentane (vortex-mixed and centrifuged at 4000 ***g*** for 2 min). The aqueous layer was extracted twice more with 500 μl of pentane each. The collected pentane layer was concentrated and directly injected into GC–MS. To determine kinetic parameters, 1 μg of protein was used in a 100 μl reaction mixture containing 25 mM Hepes (pH 7.4), 10 mM $MgCl_2$ and 0.5–25 μM FPP. The FPP was prepared by diluting 23 Ci·mmol^{-1} [1-^{3}H]FPP (PerkinElmer) 100-fold with unlabelled FPP. The mixture was incubated at 30 °C for 10 min, after which the mixture was mixed with 100 μl of stop solution (4 M NaOH and 1 M EDTA). After quenching for 10 min, 900 μl of pentane was added, vortex-mixed for 10 s and centrifuged at 15000 ***g*** for 1 min. Then, 400 μl of the pentane layer was taken and mixed with 3.5 ml of scintillation cocktail. The ^{3}H radioactivity was monitored using a Beckman LS6500 liquid scintillation counter. The Michaelis–Menten plot was created and the kinetic parameters were calculated by using the Enzyme Kinetics module in SigmaPlot 12 (Systat).

α-Bisabolol purification

For α-bisabolol purification, *MrBBS*-expressing transgenic yeast was cultured in a total of 5 litres of culture without dodecane overlay. After 3 days of culture at 30 °C, the culture medium was decanted to a separatory funnel and extracted twice with 1 litre of ethyl acetate. The combined ethyl acetate fraction was concentrated on a rotary evaporator to 2 ml, which was loaded on to a silica column (24 mm×225 mm, 15 g of silica gel 60, 40–63 μm) pre-washed with five column volumes of hexane. Then the column was eluted stepwise with 60 ml each of 0 %, 5 % and 10 % ethyl acetate in hexane. Each fraction was analysed by TLC with hexane and ethyl acetate (9:1, v/v) as elution solvent and was visualized under iodine vapour. The fractions containing α-bisabolol were combined and loaded on to a pre-coated silica gel 60 F254 plate (175–225 μm, Merck), which was eluted by hexane and ethyl acetate (9:1, v/v). The α-bisabolol-containing fraction was extracted with ethyl acetate. Evaporation of the solvent gave 34 mg of purified bisabolol suitable for spectrometric analyses.

Chemical analyses

1D and 2D NMR [^{1}H, ^{13}C, ^{1}H-^{1}H COSY, DEPT (distortionless enhancement by polarization transfer), HSQC and HMBC (heteronuclear multiple bond correlation)] experiments were conducted on a JNM-LA400 spectrometer (Jeol) with [^{2}H]chloroform $CDCl_3$ as solvent. The optical rotation was determined by using a Jasco P-1020 polarimeter (Jasco). Authentic (−)-α-bisabolol was used as standard (Sigma). To analyse sesquiterpene products from *MrBBS*-expressing yeast, the diluted dodecane layer was directly injected into GC–MS (PerkinElmer Clarus 680 GC system coupled to a PerkinElmer 600T mass spectrometer) with the following temperature programme: initial temperature of 50 °C (5-min hold), increased to 200 °C at 2 °C·min^{-1}, and ramped to 300 °C at 50 °C·min^{-1} (15 min hold). The GC column was TG-5MS (0.25 μm film thickness, 0.25 mm×30 m, Thermo Scientific). Retention times of the products were compared with those of authentic (−)-α-bisabolol, and the fragmentation pattern was searched against the NIST11 database. To identify the *in vitro* enzymatic product of MrBBS, 2 μl of pentane extract was directly analysed by GC–MS (Agilent 6890N gas chromatography system and Agilent 5975B mass spectrometer) with an authentic standard in the following temperature program: injection at 250 °C, and ramped from 40 °C to 250 °C at a rate of 10 °C·min^{-1}. The column used was DB1-MS (0.25 μm film thickness, 250 μm×30 m) and helium was used as a carrier gas with a flow rate of 1 ml·min^{-1}. For chiral analysis, a previously published GC–MS method and chiral column were used [21].

RNA isolation and expression analysis

Harvested plant material was ground in liquid nitrogen and extracted using TRIzol® reagent (Invitrogen). A 1 μg sample of total RNA was used to synthesize first-strand cDNA with the cDNA synthesis kit (J&M). Bisabolol synthase transcript level was determined using qRT-PCR (quantitative reverse transcription–PCR) on a Rotor-Gene 2000 instrument (Corbett Research) using 50 ng of cDNA with 2× QuantiMix SYBR kit (J&M) and primers 17/18. All qRT-PCRs were performed in triplicate. The endogenous actin gene was used as internal control with primers 19/20. qRT-PCR primers are listed in Supplementary Table S1. Relative gene expression was calculated using the $\Delta\Delta C_T$ method.

Transient expression in *N. benthamiana* leaves

MrBBS and its N-terminally deleted versions were PCR-amplified with specific primers (21–24) and cloned into pDONR221, and then transferred to pK7WG2D using the Gateway system (Invitrogen). The recombinant vectors were transformed into *Agrobacterium tumefaciens* LBA4404, and transformed cells were cultured overnight at 28 °C in 50 ml of LB medium containing rifampicin (20 μg·ml^{-1}) and spectinomycin (100 μg·ml^{-1}). The cultures were centrifuged at 3500 ***g*** for 10 min, and resuspended in buffer (10 mM Mes, 10 mM $MgCl_2$ and 150 μM acetosyringone, pH 5.6) to adjust the D_{600} to 0.5. The suspension was incubated further at room temperature for 8 h. The culture was infiltrated into the abaxial side of 6-week-old *N. benthamiana* leaves with a 1 ml syringe. After 4 days, leaves were harvested and ground in liquid nitrogen with a pestle and mortar, followed by vortex-mixing in ethyl acetate and sonication for 15 min. The extracts were centrifuged at 3500 ***g*** for 10 min and dehydrated with Na_2SO_4. GC–MS analysis conditions were the same as above for *in vivo* yeast characterization except for the temperature programme (1 min hold at 130 °C, linear increase to 230 °C at 10 °C·min^{-1} and subsequent linear increase to 310 °C at 20 °C·min^{-1} with a 10 min hold).

Subcellular localization of bisabolol synthase

Full-length *MrBBS* and a DNA fragment encoding its N-terminal 52 residues were amplified by PCR (primers 21–27). The PCR products were cloned into pEAQ-GFP vector [30], and infiltration experiments were performed as described above. Confocal microscopy was performed with a multi-photon confocal laser-scanning microscope (DE/LSM 510 NLO, Carl Zeiss). Infiltrated

N. benthamiana leaves were excited with a 488 nm laser at 10 %. Emission was detected between 500 and 530 nm. The chlorophyll autofluorescence was detected at 560 nm.

Bioinformatic analysis to identify candidate sesqui-TPS genes

Transcriptome data of *M. recutita* were obtained from the publicly available PhytoMetaSyn project (http://www.phytometasyn.ca). Putative sesquiterpene synthase (sesqui-TPS) genes were screened from the assembled dataset using tBLASTn. Subcellular localization of MrBBS was predicted by ChloroP (http://cbs.dtu.dk/services/ChloroP), TargetP (http://cbs.dtu.dk/services/TargetP) and PSORT (http://psort.hgc.jp/form2.html). For quantitative mapping, the 'Map reads to reference' tool in the CLC Genomics Workbench (5.5.1) was employed using a single read Illumina data. The parameters used were: mismatch cost, 2; insertion cost, 1; deletion cost, 1; length fraction, 0.8; similarity fraction, 0.98.

RESULTS

Sesquiterpene synthase isolation from chamomile cDNA

The focus of the present study was to identify (−)-α-bisabolol synthase from chamomile (*Matricaria recutita*), an Asteraceae family plant species known to synthesize (−)-α-bisabolol as one of the main floral terpene products. Using chamomile floret mRNAs, a half plate of 454 and one lane of Illumina sequencing were carried out to determine deep transcript sequences. From 454 titanium sequencing, 735 449 reads with an average length of 480 bp were generated, and 602 979 cleaned reads were assembled using the MIRA algorithm [31], yielding 44 324 contigs. From Illumina GAII sequencing, 64 608 668 reads at an average length of 108 bp were sequenced, and 54 992 498 cleaned reads with an average length of 81 bp were assembled using the Velvet algorithm [32], yielding 59 718 unique transcripts. The BLAST-searchable assembled transcript data for both 454 and Illumina data are accessible through the PhytoMetaSyn website (http://www.phytometasyn.ca) [33,34].

From these assembled transcripts, eight sesqui-TPS cDNAs encoding full-length enzymes were identified, and subsequently all eight cDNAs were PCR-cloned from chamomile floral tissues. These cDNAs were named *MrTPS1–MrTPS8*. Of these, two sesqui-TPS clones, *MrTPS3* and *MrTPS5*, displayed >99 % sequence identity with the previously reported chamomile sesqui-TPSs, and these were shown to encode (−)-germacrene D synthase and germacrene A synthase respectively [26]. Therefore these two clones were excluded from subsequent functional analysis, and the remaining six clones (*MrTPS1*, *MrTPS 2*, *MrTPS 4* and *MrTPS 6–MrTPS8*) were subjected to functional expression in yeast.

Activity screening of sesquiterpene synthases in yeast

In order to assess whether (−)-α-bisabolol synthase is present among the isolated cDNAs, the ORFs of the six clones were expressed under the *Gal1* promoter of the pESC-Leu2d plasmid in yeast [28]. The plasmid harbouring each sesqui-TPS cDNA was used to transform the EPY300 yeast strain engineered to endogenously produce an elevated level of FPP, a sesqui-TPS substrate [28,29]. Volatile terpenes produced from the transgenic yeast cultures were sequestered by dodecane overlaid on the culture, and terpenes trapped in the dodecane were analysed by GC–MS. GC–MS analyses showed that yeast strains expressing *MrTPS1*, *MrTPS4* and *MrTPS6* synthesize terpene products different from those of the vector control, demonstrating the synthesis of novel terpenes by these chamomile sesqui-TPS enzymes (Figure 2A). However, volatile product profiles of the yeast expressing *MrTPS2*, *MrTPS7* and *MrTPS8* were the same as the control (results not shown). The EI (electron impact) spectral matches of the new volatiles against the MS database suggested that the *MrTPS1*, *MrTPS4* and *MrTPS6*-expressing yeast strains synthesize α-bisabolol, bicyclogermacrene and β-farnesene respectively, as major terpene products (Figures 2C–2E). Of particular interest is the *MrTPS1*-expressing yeast strain showing a dominant peak with an EI–mass spectrum identical with that of α-bisabolol in the database. To confirm this, an authentic (−)-α-bisabolol standard was analysed by GC–MS together with the MrTPS1 product, and the MrTPS1 product showed an identical mass-fragmenting pattern and comparable retention time with those of the (−)-α-bisabolol standard (Figures 2B and 2C). Aside from the farnesol (Figure 2, peak 4) derived from the FPP substrate in yeast, α-bisabolol was a single terpene produced by MrTPS1. On the basis of this result, *MrTPS1* was named chamomile α-bisabolol synthase (*MrBBS*).

Relative expression of *MrBBS* in chamomile

A recent chemical analysis of chamomile has shown that α-bisabolol and its oxidized products, bisabolol oxide A and B, are the most abundant terpenoids in ray and disk florets among different plant tissues (63–81 % of total terpenes) [26]. It is therefore predicted that the expression of *MrBBS* is highest in chamomile florets. To determine whether *MrBBS* transcripts are most abundant in floral tissues, qRT-PCR analysis was conducted in various tissues, including three different developmental stages of flowers. qRT-PCR results showed that *MrBBS* transcripts were 24–58-fold higher in florets than in leaf (Figure 3). In different floral stages, open flowers had an approximately 2.5-fold higher level of *MrBBS* expression than in immature flowers.

In addition to qRT-PCR data, massive Illumina sequencing enabled us to compare the relative expression levels of eight *MrTPS* genes in chamomile floral tissue. To do so, approximately 32.3 million Illumina single reads were quantitatively mapped on reference sequences of the eight sesqui-TPSs. The abundance of their transcripts varied between 320 and 5500 reads per million total reads, with *MrBBS* being the most abundant transcript in chamomile floral tissue (Table 1). These expression studies showed that *MrBBS* is predominantly expressed in the open floral tissue, in which *MrBBS* is the most abundant transcript among the eight sesqui-TPSs identified.

De novo α-bisabolol production in yeast

To elucidate the stereo-configuration of α-bisabolol, it was essential to acquire a sufficient amount of MrBBS-produced α-bisabolol in high purity. Before purification, the level of α-bisabolol production from the transgenic EPY300 yeast strain was examined. In a simple shaking flask condition, when the whole culture was extracted using organic solvent, 8.1 ± 0.4 mg ($n = 5$) of α-bisabolol was produced from 1 litre of culture after 4 days of cultivation (Supplementary Figure S1A at http://www.biochemj.org/bj/463/bj4630239add.htm). Although this productivity was satisfactory, we further sought yield improvement. It has been reported that the translational fusion of soluble protein to the N-terminus of sesqui-TPS can markedly increase *in vivo* production of sesquiterpene in yeast, probably

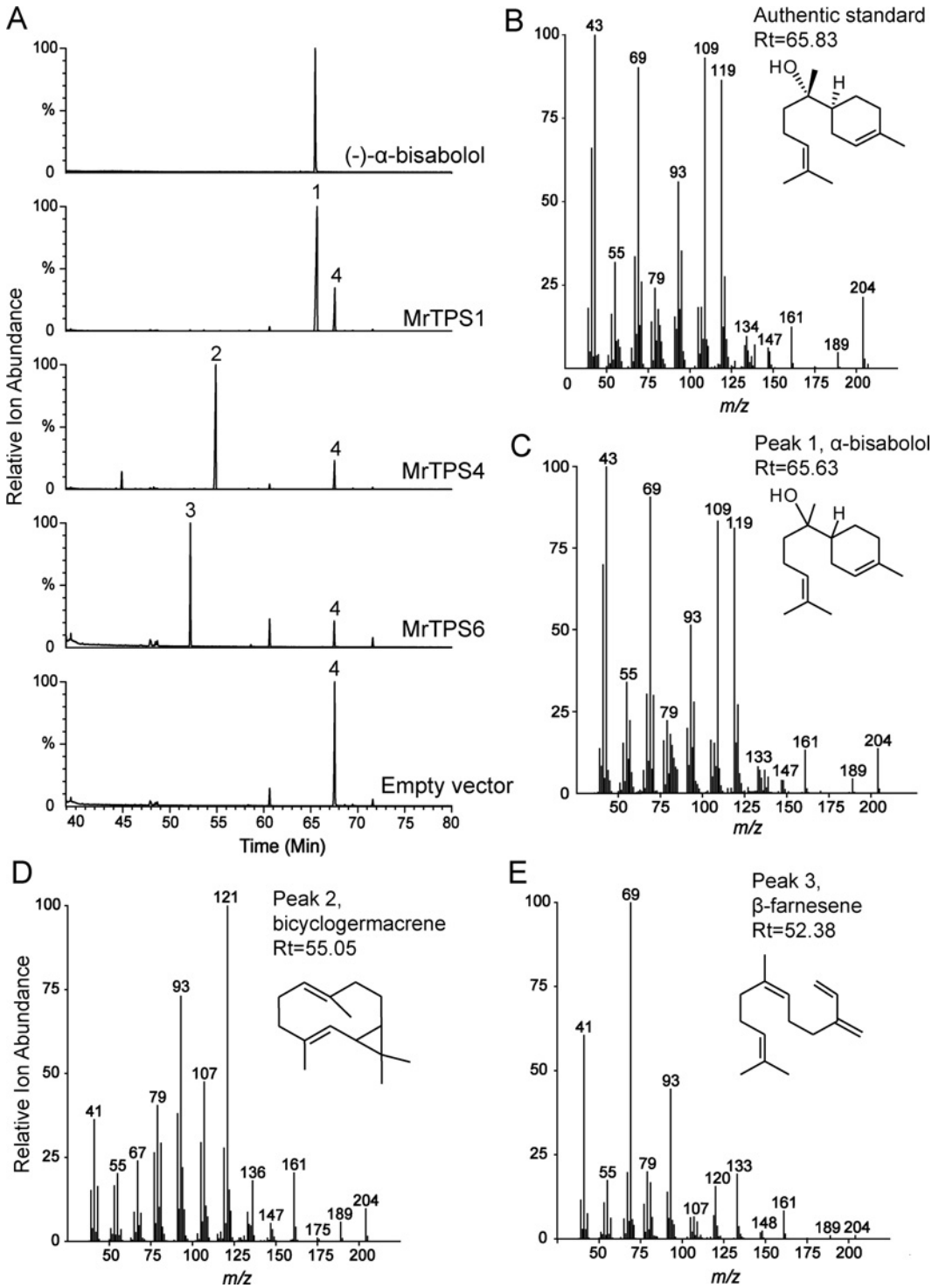

Figure 2 ***In vivo*** **screening of sesqui-TPSs isolated from chamomile in engineered yeast**

(**A**) Total ion chromatograms of authentic (−)-α-bisabolol standard, and the extracts from the yeast expressing *MrTPS1*, *MrTPS4*, *MrTPS6* and empty vector. (**B**)–(**E**) Mass spectra of (−)-α-bisabolol standard and peaks 1–3: (−)-α-bisabolol standard (**B**), peak 1 from MrTPS1 (**C**), peak 2 from MrTPS4 (**D**) and peak 3 from MrTPS6 (**E**). Peak 4 is farnesol derived from dephosphorylation of FPP. Rt, retention time.

because of increased protein solubility [35,36]. Therefore commonly used soluble protein (i.e. MBP, GST or TRX) was fused to the N-terminus of MrBBS, and the relative α-bisabolol production from the yeast lines expressing these three fusion genes were compared (Supplementary Figure S1B). MBP-fused MrBBS showed that α-bisabolol production was comparable with that of non-fused MrBBS, but GST- and TRX-fused MrBBS showed a lower level of α-bisabolol production (25 % and 32 % of non-fused MrBBS respectively) (Supplementary Figure S1C). We concluded that yeast expressing non-fused native MrBBS was

Table 1 Estimated expression levels of *MrTPS1–MrTPS8* in chamomile floral tissues

A total of 32304344 Illumina reads were used to quantitatively map *MrTPS1–MrTPS8* transcripts. In the informatics conditions used (see the Experimental section), unique and total read numbers were identical for all eight *MrTPS*s, indicating that no cross-mapping occurred in this analysis.

Name	ORF length	Unique read number	Read number per million total reads
MrTPS1 (*MrBBS*)	1719	5500	170
MrTPS2	1620	320	10
MrTPS3	1650	877	27
MrTPS4	1647	1753	54
MrTPS5	1725	4127	128
MrTPS6	1725	2739	85
MrTPS7	1650	663	21
MrTPS8	1536	346	11

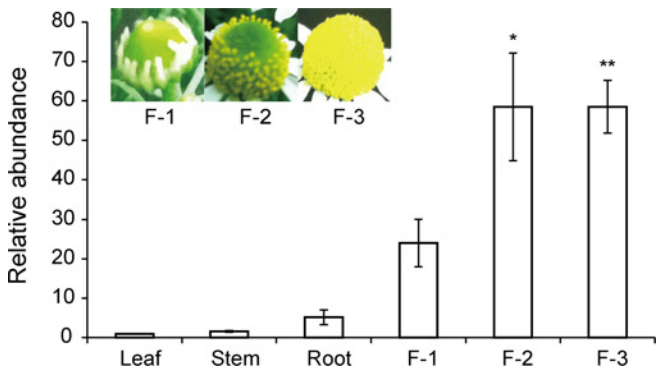

Figure 3 Relative *MrBBS* transcript levels by floral developmental stages and organs

MrBBS expression was measured relative to its transcript level in leaf (set as expression level one) by qRT-PCR ($n = 3$). Actin was used as an internal control. F-1, flower at opening stage; F-2, flower at disc floret formation stage; F-3, flower at full bloom. Statistical significance of measurements was determined by using a Student's t test (*$P \leqslant 0.05$, **$P \leqslant 0.01$) compared with F-1.

optimal for α-bisabolol production, and hence it was used for subsequent α-bisabolol purification.

Purification and structural elucidation of (−)-α-bisabolol

GC–MS data strongly suggested that the MrBBS product is α-bisabolol. To unambiguously distinguish between the four stereoisomers of α-bisabolol (Figure 1), 34 mg of α-bisabolol was purified from the whole yeast culture using a silica column, and the purified product was subjected to 1D and 2D NMR and optical rotation analysis in comparison with the authentic (−)-α-bisabolol standard. It is known that α-bisabolol and its diastereomer, *epi*-α-bisabolol, have slight but consistent differences in their ^{13}C- and ^{1}H-chemical shifts. In particular, signals of H3 and H15, and C2, C4, C6, C8 and C14 are sufficiently different between these two isomers [20,21,37]. In ^{13}C- and ^{1}H-NMR analyses, the chemical shift values of the MrBBS-product were shown to coincide completely with those of (−)-α-bisabolol standard [full ^{13}C- and ^{1}H-NMR signal assignments of MrBBS-product and (−)-α-bisabolol are given in Table 2]. Thus the MrBBS-product was clearly determined to be α-bisabolol and not *epi*-α-bisabolol. Since α-bisabolol has two enantiomers, (+)- and (−)-α-bisabolol, with identical chemical shifts, determination of the absolute configuration of MrBBS product was addressed

Table 2 ^{1}H- and ^{13}C-NMR chemical shift ([^{2}H]chloroform) values of bisabolol in the present study

NMR data here were identical with those from (−)-α-bisabolol standard.

Position	δ_{1H}	δ_{13C}
1	1.24 (m)	43.19
2a/b	1.76 (m)/1.95 (m)	27.15
3	5.35 (m)	120.76
4	–	134.39
5	1.97 (m)	31.25
6a/b	1.25 (m)/1.89 (m)	23.51
7	–	74.57
8	1.47 (m)	40.32
9	2.04 (m)	22.29
10	5.1 (m)	124.79
11	–	131.98
12	1.59 (d, $J = 1.28$Hz)	17.91
13	1.66 (s)	25.93
14	1.08 (s)	23.58
15	1.62 (s)	23.45

by optical rotation measurement. In this analysis, the observed optical rotation value, $[\alpha]^{25} - 65.8$ (ethanol), was sufficiently close to $[\alpha]^{25} - 67.6$ from the authentic (−)-α-bisabolol standard. This observation conclusively established the stereochemistry of the MrBBS product as (−)-α-bisabolol or (−)-(1*S*,7*S*)-bisabolol, which is currently commercialized as 'natural identical' α-bisabolol.

The N-terminal motif in MrBBS influences its catalytic activity

It is well established that sesqui-TPS localizes to the cytosol in agreement with its utilization of the cytosolic MVA-pathway-derived FPP. Intriguingly, however, computational prediction of subcellular location of MrBBS indicated the presence of chloroplast-targeting sequences. The TargetP and ChloroP algorithms predicted an N-terminal 52-residue plastid-targeting peptide, whereas the PSORT algorithm predicted a N-terminal 14-residue plastid-targeting peptide. These *in silico* predictions suggested possible plastidic localization of MrBBS. Therefore we investigated the function of these unusual putative plastid-targeting peptides.

First, to examine whether the N-terminal motif affects MrBBS activity *in planta*, two truncated versions of *MrBBS* were constructed and transiently expressed in *N. benthamiana* leaves. The Δ23*MrBBS* version lacked 23 residues in the characteristic signature for plastidic localization, including 11 serine and threonine amino acids. The second Δ52*MrBBS* version lacked the 52 residues containing the plastid-targeting transit peptide predicted by TargetP and ChloroP. When (−)-α-bisabolol was measured from tobacco leaves 4 days after infiltration, full-length *MrBBS*-expressing leaves accumulated ~10 μg of (−)-α-bisabolol per g of fresh weight (Figure 4A, and Supplementary Figure S2 at http://www.biochemj.org/bj/463/bj4630239add.htm). However, the leaves expressing Δ23*MrBBS* accumulated a 41-fold lower level of (−)-α-bisabolol than those expressing full *MrBBS*. From the leaves expressing Δ52*MrBBS*, no (−)-α-bisabolol was detected. These results suggested that a short N-terminal 23-residue peptide of MrBBS influenced *in planta* (−)-α-bisabolol-synthesizing activity either by targeting MrBBS to plastid or by directly affecting MrBBS activity.

Next, the plastidic localization of MrBBS was investigated by expressing the protein as a GFP fusion. Full-length MrBBS

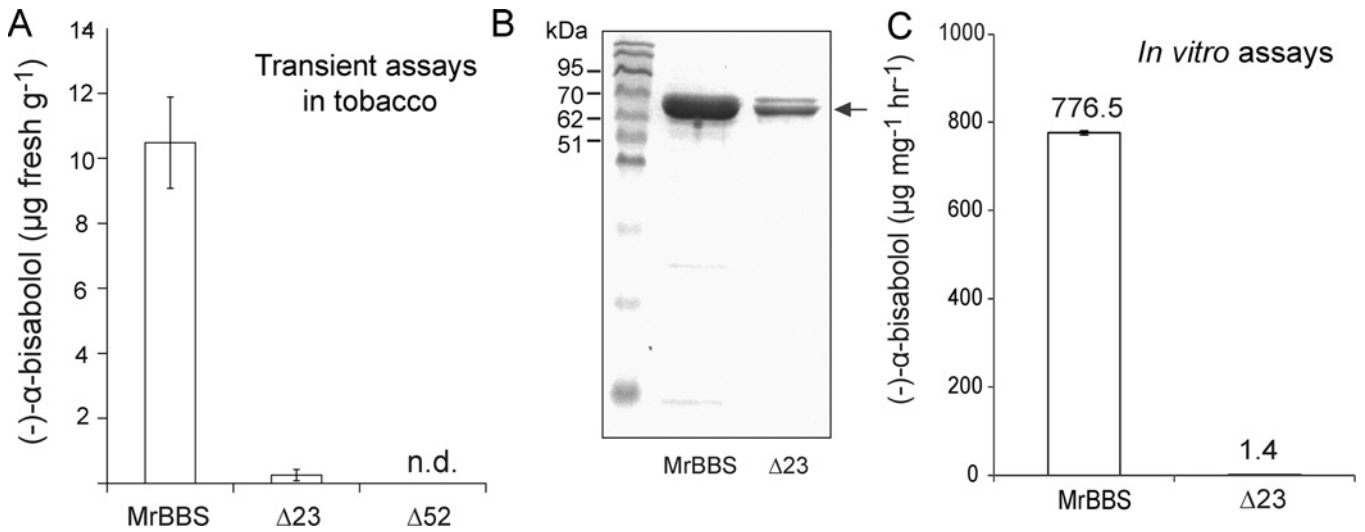

Figure 4 Characterization of truncated forms of the MrBBS enzyme

(**A**) Synthesis of (−)-α-bisabolol in tobacco leaves by transient expression of full-length *MrBBS*, 23 N-terminal residue-deleted *MrBBS* (Δ23), and 52 N-terminal residue-deleted *MrBBS* (Δ52). n.d., not detectable. (**B**) SDS/PAGE analysis of purified MrBBS and truncated form (Δ23). To compare purification yield, the same volume of cell culture and purification buffer were used. The arrow indicates purified Δ23MrBBS enzyme, and a protein band above the arrow is a contaminant from *E. coli*. Δ52MrBBS enzyme could not be detected after purification. (**C**) Specific activities of MrBBS and Δ23MrBBS in *in vitro* assays using 100 μM FPP. Results are means ± S.D. ($n = 3$).

or its N-terminal 52 residues was fused to GFP by C-terminal tagging, followed by transient expression in *N. benthamiana* leaves. Confocal microscopy, however, showed that the GFP signal did not overlap with chloroplastic autofluorescence in both the full and 52-residue-fused constructs (Figure 5). Therefore MrBBS is not localized to the plastid, but rather is localized to cytosol similarly to other sesqui-TPS enzymes despite the presence of the putative plastid-targeting motif on its N-terminus. Furthermore, it can be inferred that a short N-terminal peptide directly influences MrBBS catalytic activity.

Finally, in order to probe the role of the short N-terminal peptide on MrBBS activity, full-length *MrBBS*, Δ23*MrBBS* or Δ52*MrBBS* was expressed and purified from *E. coli* by its His_6 tag appended to the C-terminus of MrBBS. During the purification procedure, it was apparent that the truncated forms of MrBBS were either unstable or prone to aggregation in *E. coli* since significantly less recombinant enzyme could be purified from Δ23*MrBBS*-expressing bacterial cells (Figure 4B). Δ52MrBBS recombinant enzyme could not be purified from the soluble fraction, although it was present in the insoluble fraction (results not shown). When the specific activities of the full-length MrBBS and Δ23MrBBS were measured using the same amount of enzyme, Δ23MrBBS specific activity was two orders of magnitude lower than that of full-length MrBBS, indicating that the catalytic activity of Δ23MrBBS was severely compromised (Figure 4C).

Taken together, these data suggest that the N-terminal transit-peptide-like motif does not have a role in localizing MrBBS to plastids, but directly influences MrBBS stability and/or catalytic activity. A small deletion as short as 23 residues was sufficiently detrimental to MrBBS activity *in vitro* and *in planta*.

MrBBS enzyme characterization

Using purified full-length MrBBS-His_6 recombinant enzyme, kinetic properties of MrBBS were examined. MrBBS kinetic parameters were determined to have a K_m of 3.6 μM for FPP and a k_{cat} of 4.6×10^{-3}. This is comparable with other reported sesqui-TPSs (Supplementary Figure S3 at http://www.biochemj.org/bj/463/bj4630239add.htm). Kinetic parameters of Δ23MrBBS, however, could not be determined because of its negligible activity. The *in vitro* MrBBS-synthesized α-bisabolol was more carefully examined using a chiral column and the GC programme previously tuned to clearly separate different α-bisabolol isomers [21]. Besides (−)-α-bisabolol, only one other terpene, putatively assigned as β-farnesene by database search (91% spectral match), was identified in the GC–MS analysis, but this minor terpene constituted only 2% of the total terpenoids (Supplementary Figure S4 at http://www.biochemj.org/bj/463/bj4630239add.htm). No evidence of another isomer formation, other than (−)-α-bisabolol, was obtained in this chiral GC–MS analysis (Supplementary Figure S4). Therefore the MrBBS enzyme *in vitro* synthesizes enantiopure (−)-α-bisabolol with 98% terpene purity, consistent with *in vivo* data in yeast and tobacco.

DISCUSSION

(−)-α-Bisabolol, a widely added component of cosmetic products owing to its tissue-healing and -moisturizing properties, is isolated from the Brazilian candeia tree. Recent concerns over the sustainability of the candeia tree populations in Brazil have resulted in calls for the chemical synthesis of the bisabolol to meet commercial demands. However, the chemically synthesized α-bisabolol requires a costly purification process to obtain natural identical (−)-α-isomer. Therefore sustainable and economic production of (−)-α-bisabolol has become an important issue in the speciality chemical industry. In the present study, we identified a novel stereoselective (−)-α-bisabolol synthase (MrBBS) from chamomile and demonstrated its use for microbial and *in planta* (−)-α-bisabolol synthesis.

MrBBS is a unique enzyme of enantioselective (−)-α-bisabolol synthesis

One key characteristic of chamomile MrBBS, relevant to biotechnological uses, is its exclusive synthesis of

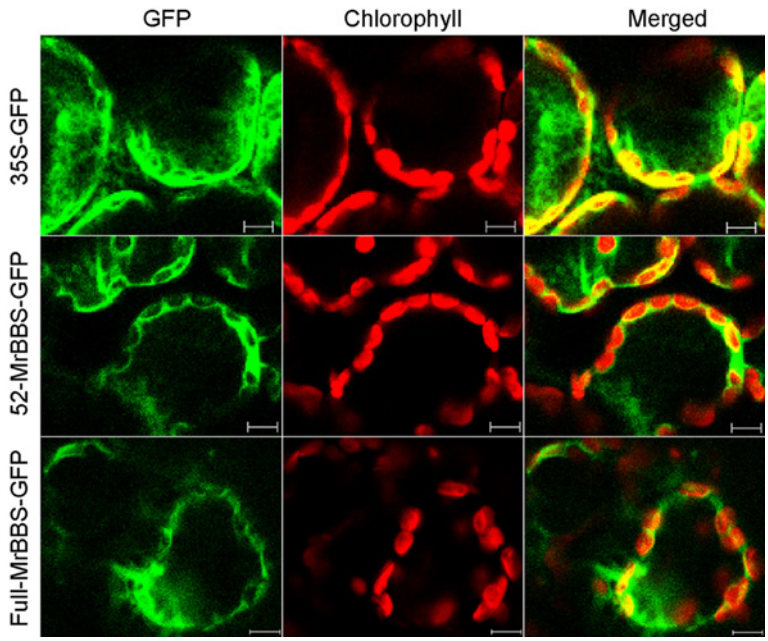

Figure 5 Subcellular localization of MrBBS in *N. benthamiana* mesophyll cells

Full-length *MrBBS* or first 52-residue fragment was C-terminally fused to GFP, and these fusion constructs were transiently expressed in *N. benthamiana* leaves. Scale bar, 10 μm.

(−)-α-bisabolol as a single terpene product. Only a negligible amount of farnesene was detected as a co-product. It has been reported that some TPSs can synthesize dozens of products. In some extreme cases, *Medicago truncatula* TPS generated 27 products and *Abies grandis* TPS generated 52 products [38,39]. With regard to TPS-mediated bisabolol synthesis, α-bisabolene synthases from Sandalwood and *Arabidopsis* synthesize α-bisabolol as a minor co-product [24,25]. Therefore, before the present study, it was reasonably postulated that (−)-α-bisabolol in chamomile was synthesized by one or more multifunctional TPSs, which could make it difficult to utilize (−)-α-bisabolol TPS for biotechnological purposes. Our MrBBS characterization data, however, showed that a single enzyme, MrBBS, is sufficient to produce a single enantioselective (−)-α-bisabolol as a major catalytic product (>98 %). Although sesqui-TPSs synthesizing α-bisabolol as a single major product have been cloned and characterized previously, these enzymes synthesized structurally different undesirable isomers (*Lippia dulcis* and *Streptomyces citricolor*) or α-bisabolol of unknown stereochemistry (*Artemisia annua*) [21–23]. At present, the catalytic feature of MrBBS [i.e. formation of a single enantiopure (−)-α-bisabolol] is unique and suitable for biotechnological synthesis of natural identical (−)-α-bisabolol. As a proof-of-concept, *MrBBS* cDNA was expressed in yeast and tobacco, and we confirmed that (−)-α-bisabolol titres of 8 mg/l of yeast culture and 10 μg/g of tobacco fresh weight can be reached. These are the first demonstrations of enantiopure (−)-α-bisabolol synthesis beyond that observed by the candeia tree and chamomile.

Proposed mechanism of (−)-α-bisabolol synthesis by MrBBS

The (1*S*)-configuration of (−)-α-bisabolol is reminiscent of the cyclization mechanism of amorphadiene synthase, in which the initial formation of (1*S*)-bisabolyl carbocation is followed by hydride shifts to form amorphadiene skeleton [40]. On the basis of this relationship, the mechanism of action of MrBBS is proposed in Figure 6. FPP is isomerized to NPP (nerolidyl diphosphate) to assume the correct conformation for the initial formation of a six-membered ring so that the overlap of the *p*-orbital at the C6 *Re* face with the C1 *p*-orbital would result in the formation of carbocation with (1*S*)-configuration. Quenching of this carbocation by a water molecule approached from the *Si* face at C7 completes the generation of (−)-α-bisabolol. We have previously cloned LdBBS [(+)-*epi*-α-bisabolol synthase from *Lippia dulcis*] [21]. For the synthesis of (+)-*epi*-α-bisabolol by LdBBS, NPP would fold in such a way that the C1 *p*-orbital overlaps with the *p*-orbital of the C6 *Si* face to result in an intermediate carbocation with (1*R*)-configuration (Figure 6). Addition of water to the cationic C7 *Si* face would lead to (1*R*,7*S*)-configuration. Therefore a comparison of 3D structures of active sites of MrBBS and LdBBS would provide a unique opportunity to identify structural elements that guide the correct folding of FPP (or NPP) required to arrive at different configurations at C1 of bisabolol.

The N-terminal motif of MrBBS influences its catalytic activity

Computational analyses of MrBBS predicted the N-terminal 52 amino acid residues to be a chloroplast-targeting transit peptide. There is precedence of chloroplast-targeted sesqui-TPS in wild tomato (*Solanum habrochaites*) [41]. In this case, the chloroplast-localized FPPS (FPP synthase) that contained the predicted plastid-localizing motif synthesizes *Z*,*Z*-FPP (or *cis*,*cis*-FPP), which is an isomer of common *E*,*E*-FPP (or *trans*,*trans*-FPP). Subsequently, chloroplast-localized sesqui-TPS catalyses the formation of santalene and bergamotene from *Z*,*Z*-FPP. Since *in silico* analyses of MrBBS sequences consistently predicted it to be a plastid-localizing enzyme, we suspected that MrBBS could also localize to the chloroplast; however, no evidence of chloroplast localization was obtained by expression of a GFP fusion to MrBBS, and MrBBS appears to localize in the cytosol. Moreover, in contrast with the *S. habrochaites* FPPS, the chamomile FPPS, identified from 454 and Illumina transcript datasets, does not possess a plastid-localizing transit peptide (results not shown). On the basis of these lines of evidence, we

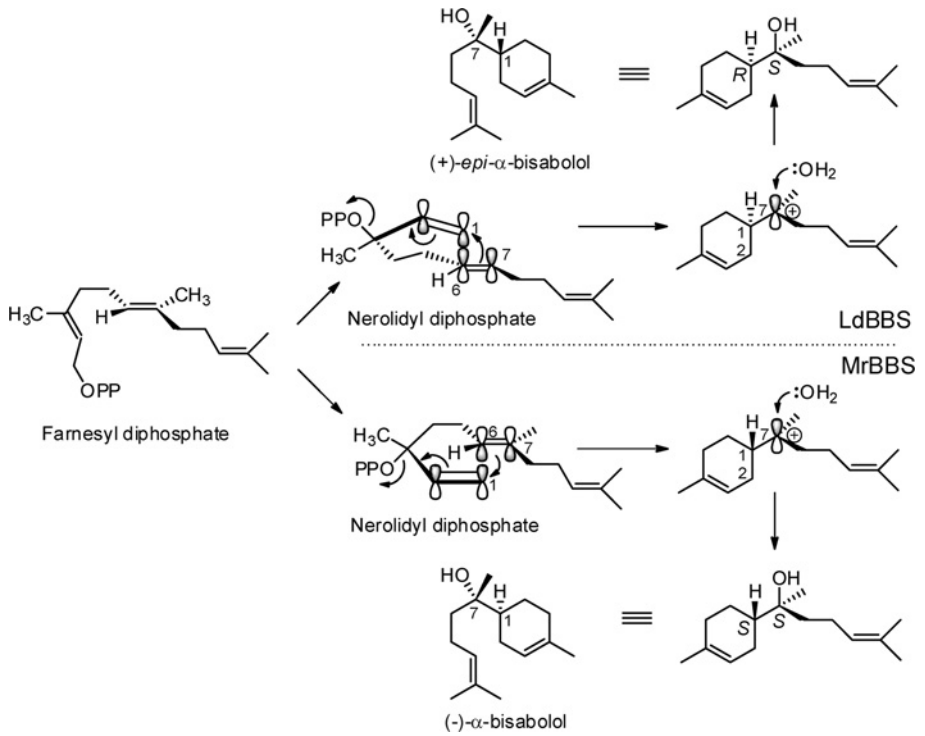

Figure 6 Proposed mechanism of MrBBS

(−)-α-Bisabolol is formed putatively via a bisabolyl cation resulting from a cyclization of neryl diphosphate isomerized from FPP by MrBBS. Addition of water to the *Si* face of bisabolyl C7 completes the reaction. The pathway leading to (+)-*epi*-α-bisabolol is shown to mark the stereochemical consequence of different NPP-folding in LdBBS as a comparison.

conclude that the computational analysis incorrectly predicted the MrBBS localization in this case.

Interestingly, the deletion of short 23 N-terminal residues in MrBBS effectively abolished its catalytic activity. On one hand, this result reinforced that the serine/threonine-rich motif is not a transit peptide since it is known that the transit peptide does not affect catalytic activity of TPS (see below). On the other hand, such a dramatic loss of sesqui-TPS activity is unexpected because the serine/threonine-rich 23-residue peptide is distal to the highly conserved $(RX)X_8W$ motif in sesqui-TPS. In mono-TPS (monoterpene synthase), this $(RX)X_8W$ motif is more refined to the RRX_8W motif, and changing the RR motif to RP or RA, or removing the RR residues in limonene synthase (mono-TPS) results in a complete loss of catalytic activity [42]. Although this RRX_8W motif has functional significance in mono-TPS, a long peptide (50–90 residues, part of which is a transit peptide) proceeding the RRX_8W motif is not required for mono-TPS catalytic activity. Hence entire residues can be removed without altering mono-TPS enzyme activity. In contrast, typical sesqui-TPS has a much shorter peptide in front of the $(RX)X_8W$ motif. For example, only five amino acids are present in front of the $(RX)X_8W$ motif in LdBBS [21] (Supplementary Figure S5 at http://www.biochemj.org/bj/463/bj4630239add.htm). Because of such an ambiguous status, the functional implication of the N-terminal sequence of sesqui-TPS has so far been overlooked.

Our data indicated that a short 23-residue peptide of MrBBS has a direct impact on its activity and may also influence the stability and/or solubility of the enzyme. It is not clear how the short peptide confers increased catalytic activity to MrBBS, although the N-terminal peptide could impose proper protein-folding and substrate-binding capability of the enzyme. Curiously, we have found that some sesqui-TPSs from the Asteraceae family also display this signature in their N-terminus [e.g. AaFAS (*A. annua* farnesene synthase) and MrTPS6/MrFAS (chamomile farnese synthase), see Supplementary Figure S5], indicating that this N-terminal signature may be retained in a small subset of sesqui-TPSs. We attempted to model the N-terminal peptide of MrBBS using the known crystal structure of 5-*epi*-aristolochene synthase in hopes to understand its role. However, X-ray crystallographic analyses of 5-*epi*-aristolochene synthases gave an indication of structural flexibility of the N-terminal region [43], which makes it difficult to implicate the role of the N-terminal region of sesqui-TPS at this moment. On the basis of our results, we propose that the serine/threonine-rich motif positioned upstream of the $(RX)X_8W$ motif does not encode a plastid-targeting transit peptide, but rather is critical for proper MrBBS function.

AUTHOR CONTRIBUTION

Young-Jin Son characterized MrBBS in yeast, purified (−)-α-bisabolol, and examined MrBBS localization. Moonhyuk Kwon characterized recombinant MrBBS from *E. coli* and plants. Dae-Kyun Ro performed *in silico* analysis, and Soo-Un Kim elucidated (−)-α-bisabolol structure. Dae-Kyun Ro and Soo-Un Kim designed the study. All authors contributed to the preparation of the paper.

ACKNOWLEDGEMENTS

We thank Mohamed Attia (University of Calgary) for *in silico* identification of *MrTPS* cDNAs and Dr Douglas Muench (University of Calgary) for help with revision of the paper.

FUNDING

This work was supported by the Next-Generation BioGreen 21 Program [Systems and Synthetic Agrobiotech Center grant number PJ009549032014], Rural Development Administration, Republic of Korea to S.-U.K. and by Genome Canada [grant number PP780422], Genome Alberta, Government of Alberta [grant number PP789067], Genome

Quebec, McGill Innovation Centre, MDEIE (Ministére du Développement Économique, Innovation et Exportation) and Canada Research Chair programme to D.-K.R.

REFERENCES

1 Buckingham, J. (2011) Dictionary of Natural Products, Chapman and Hall/CRC, London
2 Berndt, N., Hamilton, A. D. and Sebti, S. M. (2011) Targeting protein prenylation for cancer therapy. Nat. Rev. Cancer **11**, 775–791 CrossRef PubMed
3 Chappell, J. (1995) Biochemistry and molecular biology of the isoprenoid biosynthetic pathway in plants. Annu. Rev. Plant Biol. **46**, 521–547 CrossRef
4 Umehara, M., Hanada, A., Yoshida, S., Akiyama, K., Arite, T., Takeda-Kamiya, N., Magome, H., Kamiya, Y., Shirasu, K. and Yoneyama, K. (2008) Inhibition of shoot branching by new terpenoid plant hormones. Nature **455**, 195–200 CrossRef PubMed
5 Gershenzon, J. and Dudareva, N. (2007) The function of terpene natural products in the natural world. Nat. Chem. Biol. **3**, 408–414 PubMed
6 Bohlmann, J. and Keeling, C. I. (2008) Terpenoid biomaterials. Plant J. **54**, 656–669 CrossRef PubMed
7 Tholl, D. (2006) Terpene synthases and the regulation, diversity and biological roles of terpene metabolism. Curr. Opin. Plant Biol. **9**, 297–304 CrossRef PubMed
8 Bohlmann, J., Meyer-Gauen, G. and Croteau, R. (1998) Plant terpenoid synthases: molecular biology and phylogenetic analysis. Proc. Natl. Acad. Sci. U.S.A. **95**, 4126–4133 CrossRef PubMed
9 Cane, D. E. (1990) Enzymic formation of sesquiterpenes. Chem. Rev. **90**, 1089–1103 CrossRef
10 Kirby, J. and Keasling, J. D. (2009) Biosynthesis of plant isoprenoids: perspectives for microbial engineering. Annu. Rev. Plant Biol. **60**, 335–355 CrossRef PubMed
11 Singh, O., Khanam, Z., Misra, N. and Srivastava, M. K. (2011) Chamomile (*Matricaria chamomilla* L.): an overview. Pharmacogn. Rev. **5**, 82–95 CrossRef PubMed
12 Jakovlev, V., Isaac, O., Thiemer, K. and Kunde, R. (1979) Pharmacological investigations with compounds of chamomile. ii. New investigations on the antiphlogistic effects of (−)-α-bisabolol and bisabolol oxides. Planta Med. **35**, 125–140 CrossRef PubMed
13 Vuorela, H., Holm, Y., Hiltunen, R., Harvala, T. and Laitinen, A. (2006) Extraction of the volatile oil in chamomile flowerheads using supercritical carbon dioxide. Flavour Fragrance J. **5**, 81–84 CrossRef
14 de Souza, A. T., Benazzi, T. L., Grings, M. B., Cabral, V., da Silva, E. A., Cardozo-Filho, L. and Antunes, O. A. C. (2008) Supercritical extraction process and phase equilibrium of Candeia (*Eremanthus erythropappus*) oil using supercritical carbon dioxide. J. Supercrit. Fluids **47**, 182–187 CrossRef
15 Bhatia, S. P., McGinty, D., Letizia, C. S. and Api, A. M. (2008) Fragrance material review on α-bisabolol. Food Chem. Toxicol. **46**, S72–S76 CrossRef PubMed
16 Brehm-Stecher, B. F. and Johnson, E. A. (2003) Sensitization of *Staphylococcus aureus* and *Escherichia coli* to antibiotics by the sesquiterpenoids nerolidol, farnesol, bisabolol, and apritone. Antimicrob. Agents Chemother. **47**, 3357–3360 CrossRef PubMed
17 Forrer, M., Kulik, E. M., Filippi, A. and Waltimo, T. (2013) The antimicrobial activity of α-bisabolol and tea tree oil against *Solobacterium moorei*, a Gram-positive bacterium associated with halitosis. Arch. Oral Biol. **58**, 10–16 CrossRef PubMed
18 Russell, K. and Jacob, S. E. (2010) Bisabolol. Dermatitis **21**, 57–58 PubMed
19 Clark, A., Khweiss, N., Salazar, L. and Verdadero, L. (2011) Promoting sustainability in the value chain of natural bisabolol, a Brazilian rainforest product http://www.iri.usp.br/documentos/rel_Columbia_11.pdf
20 Chen, X. J., Archelas, A. and Furstoss, R. (1993) The first examples for preparative-scale enantioselective or diastereoselective epoxide hydrolyses using microorganisms: an unequivocal access to all four bisabolol stereoisomers. J. Org. Chem. **58**, 5528–5532 CrossRef
21 Attia, M., Kim, S. U. and Ro, D. K. (2012) Molecular cloning and characterization of (+)-*epi*-α-bisabolol synthase, catalyzing the first step in the biosynthesis of the natural sweetener, hernandulcin, in *Lippia dulcis*. Arch. Biochem. Biophys. **527**, 37–44 CrossRef PubMed
22 Nakano, C., Kudo, F., Eguchi, T. and Ohnishi, Y. (2011) Genome mining reveals two novel bacterial sesquiterpene cyclases: (−)-germacradien-4-ol and (−)-*epi*-α-bisabolol synthases from *Streptomyces citricolor*. ChemBioChem **12**, 2271–2275 CrossRef PubMed
23 Li, J. X., Fang, X., Zhao, Q., Ruan, J. X., Yang, C. Q., Wang, L. J., Miller, D. J., Faraldos, J. A., Allemann, R. K., Chen, X. Y. and Zhang, P. (2013) Rational engineering of plasticity residues of sesquiterpene synthases from *Artemisia annua*: product specificity and catalytic efficiency. Biochem. J. **451**, 417–426 CrossRef PubMed
24 Jones, C. G., Moniodis, J., Zulak, K. G., Scaffidi, A., Plummer, J. A., Ghisalberti, E. L., Barbour, E. L. and Bohlmann, J. (2011) Sandalwood fragrance biosynthesis involves sesquiterpene synthases of both the terpene synthase (TPS)-a and TPS-b subfamilies, including santalene synthases. J. Biol. Chem. **286**, 17445–17454 CrossRef PubMed
25 Ro, D. K., Ehlting, J., Keeling, C. I., Lin, R., Mattheus, N. and Bohlmann, J. (2006) Microarray expression profiling and functional characterization of AtTPS genes: duplicated *Arabidopsis thaliana* sesquiterpene synthase genes At4g13280 and At4g13300 encode root-specific and wound-inducible (*Z*)-γ-bisabolene synthases. Arch. Biochem. Biophys. **448**, 104–116 CrossRef PubMed
26 Irmisch, S., Krause, S. T., Kunert, G., Gershenzon, J., Degenhardt, J. and Kollner, T. G. (2012) The organ-specific expression of terpene synthase genes contributes to the terpene hydrocarbon composition of chamomile essential oils. BMC Plant Biol. **12**, 84 PubMed
27 Gietz, R. D. and Schiestl, R. H. (2007) High-efficiency yeast transformation using the LiAc/SS carrier DNA/PEG method. Nat. Protoc. **2**, 31–34 CrossRef PubMed
28 Ro, D. K., Ouellet, M., Paradise, E. M., Burd, H., Eng, D., Paddon, C. J., Newman, J. D. and Keasling, J. D. (2008) Induction of multiple pleiotropic drug resistance genes in yeast engineered to produce an increased level of anti-malarial drug precursor, artemisinic acid. BMC Biotechnol. **8**, 83 CrossRef PubMed
29 Ro, D. K., Paradise, E. M., Ouellet, M., Fisher, K. J., Newman, K. L., Ndungu, J. M., Ho, K. A., Eachus, R. A., Ham, T. S., Kirby, J. et al. (2006) Production of the antimalarial drug precursor artemisinic acid in engineered yeast. Nature **440**, 940–943 CrossRef PubMed
30 Sainsbury, F., Thuenemann, E. C. and Lomonossoff, G. P. (2009) pEAQ: versatile expression vectors for easy and quick transient expression of heterologous proteins in plants. Plant Biotechnol. J. **7**, 682–693 CrossRef PubMed
31 Chevreux, B., Pfisterer, T., Drescher, B., Driesel, A. J., Muller, W. E., Wetter, T. and Suhai, S. (2004) Using the miraEST assembler for reliable and automated mRNA transcript assembly and SNP detection in sequenced ESTs. Genome Res. **14**, 1147–1159 CrossRef PubMed
32 Zerbino, D. R. and Birney, E. (2008) Velvet: algorithms for *de novo* short read assembly using de Bruijn graphs. Genome Res. **18**, 821–829 CrossRef PubMed
33 Facchini, P. J., Bohlmann, J., Covello, P. S., De Luca, V., Mahadevan, R., Page, J. E., Ro, D. K., Sensen, C. W., Storms, R. and Martin, V. J. (2012) Synthetic biosystems for the production of high-value plant metabolites. Trends Biotechnol. **30**, 127–131 CrossRef PubMed
34 Xiao, M., Zhang, Y., Chen, X., Lee, E. J., Barber, C. J., Chakrabarty, R., Desgagne-Penix, I., Haslam, T. M., Kim, Y. B., Liu, E. et al. (2013) Transcriptome analysis based on next-generation sequencing of non-model plants producing specialized metabolites of biotechnological interest. J. Biotechnol. **166**, 122–134 CrossRef PubMed
35 Gopfert, J. C., Macnevin, G., Ro, D. K. and Spring, O. (2009) Identification, functional characterization and developmental regulation of sesquiterpene synthases from sunflower capitate glandular trichomes. BMC Plant Biol. **9**, 86 PubMed
36 Nguyen, T. D., MacNevin, G. and Ro, D. K. (2012) *De novo* synthesis of high-value plant sesquiterpenoids in yeast. Methods Enzymol. **517**, 261–278 CrossRef PubMed
37 Hashidoko, Y., Endoh, K., Kudo, T. and Tahara, S. (2000) (+)-4-*epi*-α-bisabolol as a major sesquiterepene constituent in the leaves of two *Rosa rugosa* hybrids, Martin Frobisher and Vanguard. Biosci. Biotechnol. Biochem. **64**, 907–910 CrossRef PubMed
38 Garms, S., Kollner, T. G. and Boland, W. (2010) A multiproduct terpene synthase from *Medicago truncatula* generates cadalane sesquiterpenes via two different mechanisms. J. Org. Chem. **75**, 5590–5600 CrossRef PubMed
39 Steele, C. L., Crock, J., Bohlmann, J. and Croteau, R. (1998) Sesquiterpene synthases from grand fir (*Abies grandis*): comparison of constitutive and wound-induced activities, and cDNA isolation, characterization, and bacterial expression of δ-selinene synthase and γ-humulene synthase. J. Biol. Chem. **273**, 2078–2089 CrossRef PubMed
40 Kim, S.-H., Heo, K., Chang, Y.-J., Park, S.-H., Rhee, S.-K. and Kim, S.-U. (2006) Cyclization mechanism of amorpha-4,11-diene synthase, a key enzyme in artemisinin biosynthesis. J. Nat. Prod. **69**, 758–762 CrossRef PubMed
41 Sallaud, C., Rontein, D., Onillon, S., Jabes, F., Duffe, P., Giacalone, C., Thoraval, S., Escoffier, C., Herbette, G., Leonhardt, N. et al. (2009) A novel pathway for sesquiterpene biosynthesis from *Z*,*Z*-farnesyl pyrophosphate in the wild tomato *Solanum habrochaites*. Plant Cell **21**, 301–317 CrossRef PubMed
42 Williams, D. C., McGarvey, D. J., Katahira, E. J. and Croteau, R. (1998) Truncation of limonene synthase preprotein provides a fully active 'pseudomature' form of this monoterpene cyclase and reveals the function of the amino-terminal arginine pair. Biochemistry **37**, 12213–12220 CrossRef PubMed
43 Starks, C. M., Back, K., Chappell, J. and Noel, J. P. (1997) Structural basis for cyclic terpene biosynthesis by tobacco 5-*epi*-aristolochene synthase. Science **277**, 1815–1820 CrossRef PubMed

Received 5 March 2014/16 July 2014; accepted 22 July 2014
Published as BJ Immediate Publication 22 July 2014, doi:10.1042/BJ20140306

Biochem. J. (2014) **463**, 239–248 (Printed in Great Britain) doi:10.1042/BJ20140306

online data

SUPPLEMENTARY ONLINE DATA

Enantioselective microbial synthesis of the indigenous natural product (−)-α-bisabolol by a sesquiterpene synthase from chamomile (*Matricaria recutita*)

Young-Jin SON*, Moonhyuk KWON†, Dae-Kyun RO†[1] and Soo-Un KIM*‡[1]

*Department of Agricultural Biotechnology and Research Institute of Agriculture and Life Sciences, Seoul National University, Seoul 151-921, South Korea
†Department of Biological Sciences, University of Calgary, Calgary, Canada, T2N 1N4
‡School of Gardening and Horticulture, Yangtze University, Jingzhou, Hubei 434023, China

Table S1 Primers used in the present study

Number	Primer	Sequence (5′→3′)	Usage
1	MrTPS1-F	GACCGGATCCAACATGTCAACTTTATCAGTTTCTACTCCTTCC	pESC-Leu2d
2	MrTPS1-R	GGTCTCTAGACTAGACAATCATAGGGTGAACGAAGAG	pESC-Leu2d
3	MrTPS2-F	GACCGGATCCAACATGGTTTCGATGTTTGCCCAAC	pESC-Leu2d
4	MrTPS2-R	GGTCCTCGAGTCAGACACTTCCACGACTATGATCAC	pESC-Leu2d
5	MrTPS4-F	GACCGGGCCCAACATGGCTCCACAACAAGAGGAAGTC	pESC-Leu2d
6	MrTPS4-R	GGTCTCTAGATCAAATAGTCATAGGGTGAACGAATGAG	pESC-Leu2d
7	MrTPS6-F	GACCGGGCCCAACATGTCAACTATTCCTGTTTCTAGTGTTTCTTTC	pESC-Leu2d
8	MrTPS6-R	GGTCTCTAGATTAGATAACCATAGGGTGAACGAAGTACG	pESC-Leu2d
9	MrTPS7-F	GACCGGGCCCAACATGAGCACAAAACAAGAAGAGAATATCC	pESC-Leu2d
10	MrTPS7-R	GGTCTCTAGATCAGACGATCATAGGATGAACGAG	pESC-Leu2d
11	MrTPS8-F	GACCGGATCCAACATGATGATCAACAACTGTGTTACACGGA	pESC-Leu2d
12	MrTPS8-R	GGTCCTCGAGTTAAAACATGTAGTTTATATATTCCTCGATGAAAGG	pESC-Leu2d
13	MrTPS1-F	TAAGAAGGAGATATACATATGTCAACTTTATCAGTTTCTACTCCTTC	pET21
14	Δ23aa-F	TAAGAAGGAGATATACATATGACGAAGCAACATGTTACTCGC	pET21
15	Δ52aa-F	TAAGAAGGAGATATACATATGGTAGCTACTGAGAAACAGCTAATCG	pET21
16	MrTPS1-R	TCAGTGGTGGTGGTGGTGGTGCTCGAGGACAATCATAGGGTGAACGAAGAG	pET21
17	MrTPS1-F	TTATGTTGCCCGGGATGACG	qPCR
18	MrTPS1-R	TTGTTCCTCCTTGTGGGTGG	qPCR
19	Actin-F	GCTAACAGGGAAAAGATGACTC	qPCR
20	Actin-R	ACTGGCATAAAGAGAAAGCACG	qPCR
21	MrTPS1-F	AAAAAAGCAGGCTCTATGTCAACTTTATCAGTTTCTACTCCTTCC	pK7WG2D
22	Δ23aa-F	AAAAAAGCAGGCTCTATGACGAAGCAACATGTTACTCGCA	pK7WG2D
23	Δ52aa-F	AAAAAAGCAGGCTCTATGGTAGCTACTGAGAAACAGCTAATCGAG	pK7WG2D
24	MrTPS1-R	CAAGAAAGCTGGGTCCTAGACAATCATAGGGTGAACGAAGAGC	pK7WG2D
25	MrTPS1-F	TTCTGCCCAAATTCGCGACCGGTATGTCAACTTTATCAGTTTCTACTCCTTC	pEAQ-HT-GFP
26	MrTPS1-R	TCTCCTTTGCTAGTCATACCGGTGACAATCATAGGGTGAACGAAGAG	pEAQ-HT-GFP
27	52aa-R	TCTCCTTTGCTAGTCATACCGGTATTGGATTTCTCCTTATATTCAAGAAA	pEAQ-HT-GFP
28	MBP-F	CCGGATCCAACATGAAAATCGAAGAAGGTAAACTG	pESC-Leu2d
29	MBP-R	TTACGGATCCTTCCGAGCTCGAATTAGTCTG	pESC-Leu2d
30	GST-F	CCGGATCCAACATGTCCCCTATACTAGGTTATTGG	pESC-Leu2d
31	GST-R	TTACGGATCCATCCGATTTTGGAGGATGG	pESC-Leu2d
32	Trx-F	CTATAGGGCCCATGAGCGATAAAATTATTCACC	pESC-Leu2d
33	Trx-R	GCTTACTCGAGGGCCAGGTTAGCGTCGAGGAAC	pESC-Leu2d

[1] Correspondence may be addressed to either of these authors (email soounkim@snu.ac.kr or daekyun.ro@ucalgary.ca).

Nucleotide sequence of identified *Matricaria recutita* sesquiterpene synthases have been submitted to the DDBJ, EMBL, GenBank® and GSDB Nucleotide Sequence Databases with accession numbers: KJ020282 [MrTPS1, (−)-α-bisabolol synthase], KJ020284 (MrTPS4, bicyclogermacrene synthase) and KJ020283 (MrTPS6, β-farnesene synthase).

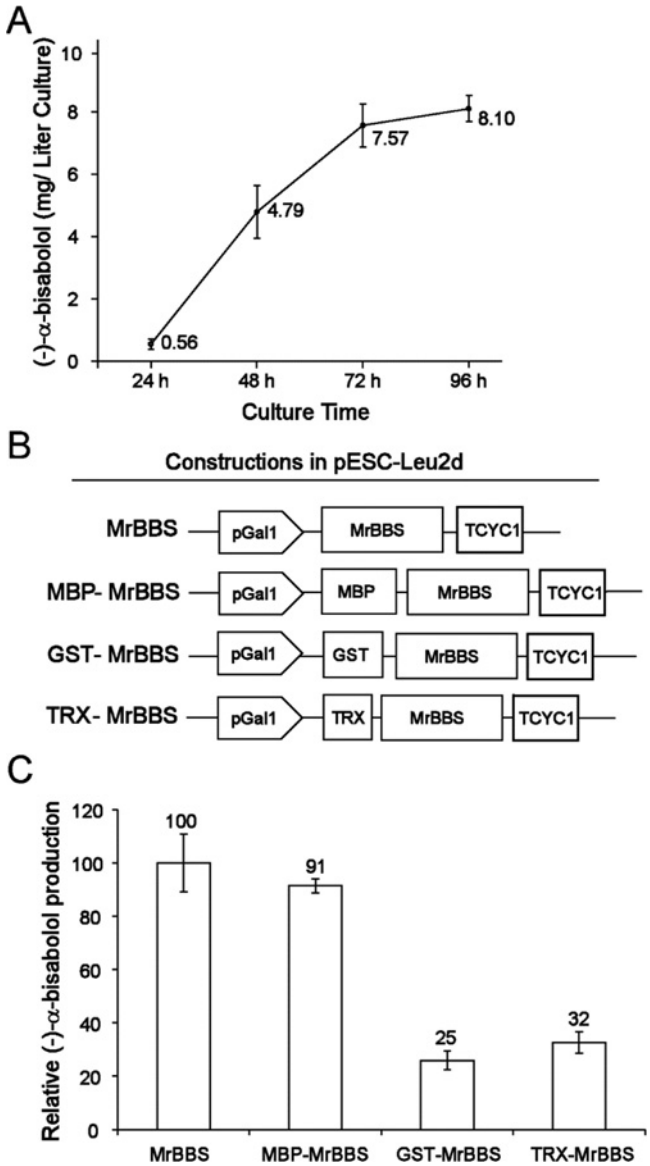

Figure S1 ***In vivo*** **(−)-α-bisabolol production in yeast**

(**A**) Quantitative synthesis of (−)-α-bisabolol from transgenic yeast over 4 days. (**B**) Schematic representation of fusion constructs. (**C**) (−)-α-bisabolol productions from the yeast expressing various MrBBS species fused with soluble proteins at its N-terminus. Results are means±S.D. ($n = 3$).

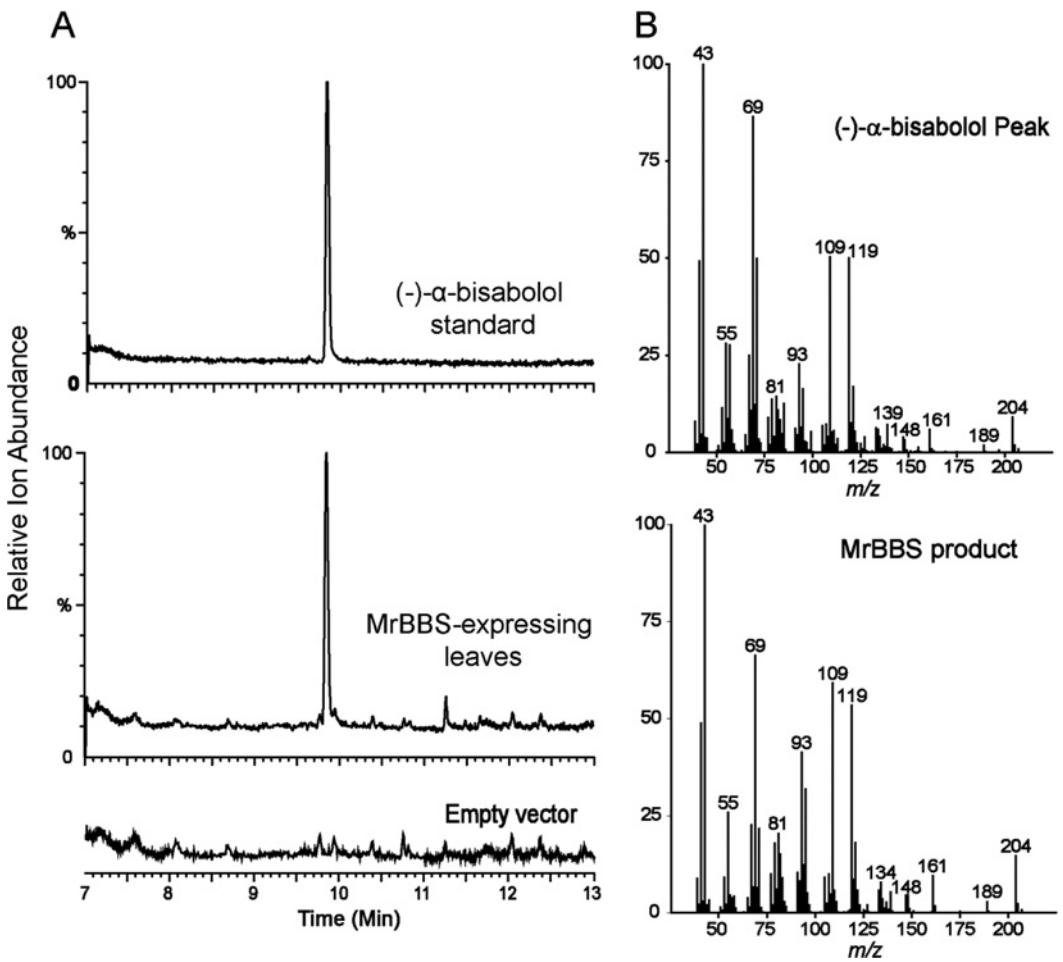

Figure S2 Synthesis of (−)-α-bisabolol by transient expression of *MrBBS* in tobacco leaves

(**A**) GC–MS detection of (−)-α-bisabolol from the tobacco leaves expressing *MrBBS* in comparison with standard and empty vector control. (**B**) Comparison of ion fragmenting patterns of the standard and MrBBS product.

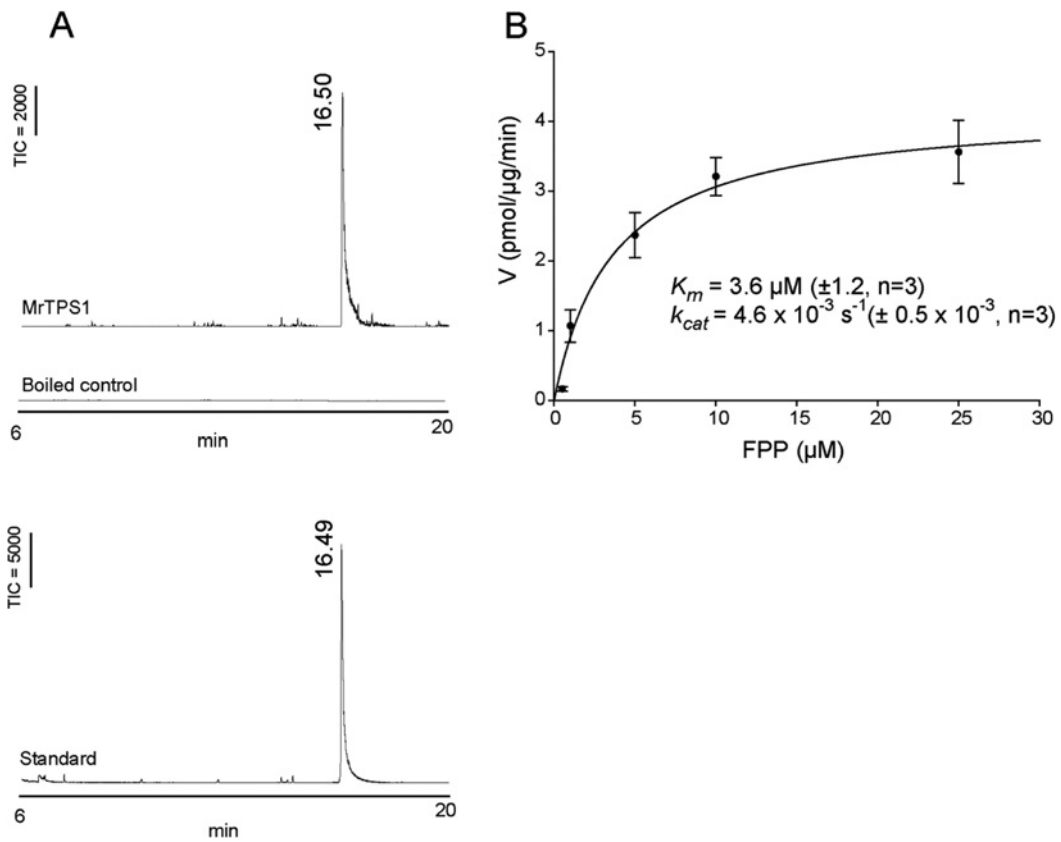

Figure S3 ***In vitro*** **kinetic analysis of MrBBS recombinant enzyme**

(**A**) GC–MS analysis of MrBBS product from *in vitro* assays. (**B**) Michaelis–Menten kinetics plot for MrBBS recombinant enzyme with FPP substrate ranging from 0.5 to 25 μM. Results are means±S.D.

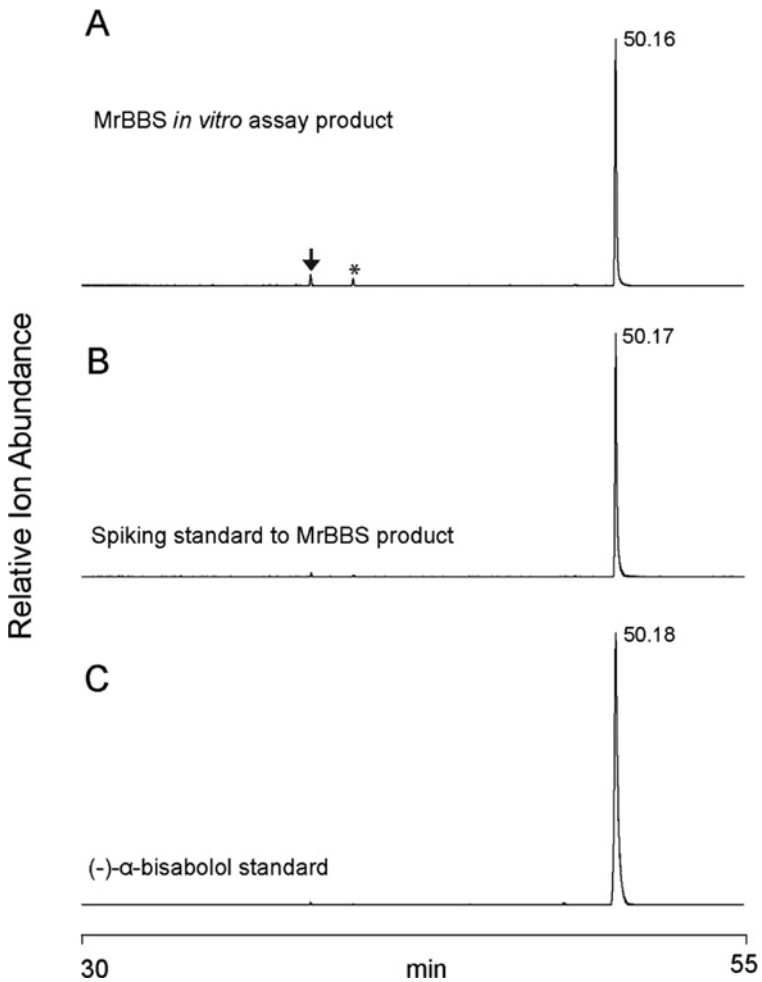

Figure S4 Chiral column analysis of *in vitro* MrBBS product

GC–MS separation of (**A**) MrBBS enzymatic product, (**B**) 1:1 mixture of MrBBS product and (−)-α-bisabolol standard, and (**C**) (−)-α-bisabolol standard. The chiral GC–MS method was optimized to separate α-bisabolol isomers [1]. The peak labelled with an arrow was identified as β-farnesene by a database spectral search. However, the peak labelled with an asterisk was not identifiable using the database and did not display the mass fragmenting pattern characteristic to sesquiterpenes.

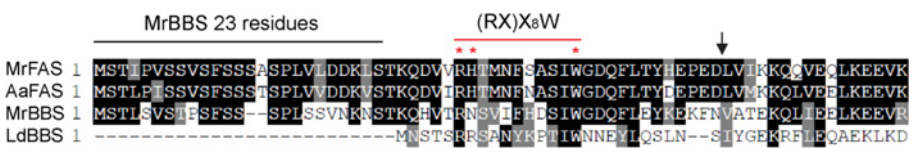

Figure S5 Comparison of N-terminal sequences of the sesquiterpene synthases related to MrBBS

The conserved (RX)X_8W motif is labelled in red with asterisks to indicate RX and W; the 23-residue N-terminal domain is marked by a black line; the first 52-residue peptide is marked by an arrow. MrFAS, chamomile β-farnesene synthase (MrTPS6) (GenBank® accession number KJ020283); AaFAS, *Artemisia annua* β-farnesene synthase (GenBank® accession number ADT64306); MrBBS, chamomile (−)-α-bisabolol synthase (MrTPS1) (GenBank® accession number KJ020282); LdBBS, *Lippia dulcis* (+)-*epi*-α-bisabolol synthase (GenBank® accession number JQ731636).

REFERENCE

1 Attia, M., Kim, S. U. and Ro, D. K. (2012) Molecular cloning and characterization of (+)-*epi*-α-bisabolol synthase, catalyzing the first step in the biosynthesis of the natural sweetener, hernandulcin, in *Lippia dulcis*. Arch. Biochem. Biophys. **527**, 37–44 CrossRef PubMed

Received 5 March 2014/16 July 2014; accepted 22 July 2014
Published as BJ Immediate Publication 22 July 2014, doi:10.1042/BJ20140306